



Thermodynamic and structural changes of various intermetallic compounds during extended cycling in closed systems

M. Wanner*, G. Friedlmeier, G. Hoffmann, M. Groll

Institut für Kernenergetik und Energiesysteme (IKE), University of Stuttgart, Pfaffenwaldring 31, D-70569 Stuttgart, Germany

Abstract

The application-relevant AB₅-type intermetallic compounds LmNi_{4.85}Sn_{0.15}, LmNi_{4.49}Co_{0.1}Mn_{0.205}Al_{0.205} and LmNi_{4.08}Mn_{0.62}Al_{0.1}Co_{0.2} underwent about 90 000 thermally induced hydrogen absorption–desorption cycles in closed systems at different cycling temperatures and pressures. Depending on the individual rates of decay, regeneration procedures were carried out several times. After the half time and after the end of cycling additional experimental techniques were employed in order to determine possible structural and stoichiometric changes. Among these X-ray powder diffractometry, magnetization, scanning electron microscopy including EDX and thermal desorption spectroscopy were utilized. Besides the degradation behaviour of each material, new results are presented about the degradation phenomena (structural changes, disproportionation) and a comparison is given of various regeneration procedures.

Keywords: AB₅-type alloys; Cyclic Stability; Degradation; Disproportionation

1. Introduction

Metal hydrides are very promising working media for application in thermodynamic machines such as heat transformers, heat pumps and cooling devices [1–4]. To obtain efficient performance, especially high power output per metal hydride inventory, the time needed for an absorption–desorption cycle should be short, typically not exceeding 15 min. Thus during the lifetime of such thermodynamic machines the alloys are (de-)hydrogenated of the order of half a million times.

To study the long-term cycling behaviour, three AB₅-materials were tested which had been chosen for use in a two-stage heat transformer [3–6] under application-relevant temperatures and pressures. Even though the alloys were cycled in a closed system where contamination problems should not occur, considerable losses of the reversible hydrogen capacity were observed due to intrinsic changes in the material.

The goals of the presented work were to improve the knowledge of the processes of degradation and regeneration of hydride forming alloys on the microscopic scale and to find out how the expected degradation phenomena can be dealt with from a technical point of view.

Several investigations of the cyclic stability have already been carried out [7–10], but in none of them has a comparably high number of cycles been reached. Furthermore the presented life-time cycling experiments are the first systematic ones where the influence of the parameters temperature and pressure has been studied. In addition, several regeneration procedures (varying time, temperature and pressure) were tested to recover the initial hydrogen capacity.

In all three materials under consideration a lanthanum-rich misch-metal consisting mainly of lanthanum and neodymium is used as the so-called A component of the alloy.

2. Experimental details

2.1. Cycling device

The cycling device has been described in detail elsewhere [11]. Six materials can be cycled independently at different cycling conditions (cycling period, pressure, temperature) in closed systems. The cycling device contains four reactors for each material (sample masses about 70–120 g). This makes it possible to remove some single reactors in order to thoroughly investigate the cycled samples outside the apparatus.

*Corresponding author.

2.2. Pressure-composition isotherms and thermal desorption spectroscopy

The reactors of the cycling device can be installed on the dynamic pressure-composition isotherms (PCI) device that has been described elsewhere [12] without exposing the sample to the air. Besides measuring dynamic PCIs of several samples of each material (as-delivered, degraded, regenerated) this device could also be used for thermal desorption spectroscopy (TDS) because it contains all the necessary experimental components (viz. pressure difference transducer, programmable furnace, hydrogen reservoir, valves, automatic data acquisition unit). For the TDS experiments a heating rate of 3 K min^{-1} was chosen. The hydrogen pressure in the connected vessel rose from the initial value of 1 Pa to the maximum value of about 20 kPa at the end of the heating ramp.

The hydrogen content of the samples is determined with a volumetric method. The mass flow to and from the samples varied from 1 to $4 \text{ cm}_n^3 \text{ min}^{-1}$.

2.3. Further experimental techniques

In order to thoroughly characterize the changes of the materials after extended cycling, additional experimental techniques were employed. X-ray diffraction patterns were taken on a SIEMENS D 5000 diffractometer. Particle size distribution analysis was performed with a laser-granulometer HR 850 of CILAS-ALCATEL. SEM and EDX-analysis were carried out on a DS 130 scanning electron microscope of ISI.

2.4. Regeneration procedures

In principle all that is needed for a regeneration is a programmable furnace and a vacuum pump. Depending on

the desired temperatures and other restrictions, the original hydrogen capacity was recovered in situ, in the PCI device (via TDS) or in an external furnace.

3. Results and discussion

Results of cycling tests with up to about 45 000 cycles have already been presented in [11]. In the following the results of 45 000–95 000 cycles are presented. Some previous results are mentioned to allow essential comparisons.

3.1. $\text{LaNi}_{4.85}\text{Sn}_{0.15}$ (material A)

Table 1 gives a short summary of what happened during the three-year cycling of material A. Fig. 1 shows the reversible system capacity Δx_{sys} , the absorption temperature T_{min} and the desorption temperature T_{max} as a function of the number of cycles. Δx_{sys} is the amount of hydrogen which can be exchanged between the hydrogen reservoir and the intermetallic compound under the given cycling conditions. In the first ten thousand cycles of the second cycling period (i.e. cycles no. 31 590–94 560) the degradation rate ($1.9 \times 10^{-5} \text{ H/M}$ per cycle) is only half as big as in the first period due to less severe cycling conditions. The degradation comes to a stop at a value of $\Delta x_{\text{sys}} = 0.39 \text{ H/M}$ after about 80 000 cycles.

The PCIs shown in Fig. 2 indicate severe changes in the thermodynamic properties. The degraded samples have no longer a plateau region. However plateau slope and hydrogen capacity can be fully recovered by regeneration. The equilibrium pressure after regeneration ($p_{\text{eq,reg}} \sim 0.8 \text{ MPa}$) seems to be reproducible but the initial value ($p_{\text{eq},0} = 0.52 \text{ MPa}$) could not be achieved although the reason for that is not quite clear (as we could not find significant

Table 1
Summary of data and experiments

Material	A	B	C
Manufacturer	GfE, Nürnberg, Germany	GfE, Nürnberg, Germany	GfE, Nürnberg, Germany
Particle size, as delivered (μm)	31	30	32
Reaction enthalpyabs./des. (kJ/mol H_2)	−28.6/29.7	−33.1/33.9	−39.9/42.2
Initial sample mass (g)	120.1	72	72
Number of cycles	94 560	96 280	96 480
Regenerations at cycle no.	31 590 (530/22.5/1)	33 850 (450/72/1)	14 670 (380/8.5/1)
(temperature ($^{\circ}\text{C}$)/	94 560 (500/24/1)	96 280 (500/24/1)	25 340 (450/25/1)
time (h)/pressure (Pa))			38 920 (450/19/1)
			46 000 (450/30/1)
			96 480 (650/3/1)
2 of 4 reactors removed at cycle no.	31 590	33 850	25 340
1 of 2 remaining reactors removed at cycle no.			46 000
Investigations at cycle no.	31 590: XRPD, REM/EDX, Magnetization, PCI, TDS, Laser-granulometry	33 850: XRPD, REM/EDX, Magnetization, PCI, TDS, Laser-granulometry	25 340: XRPD, REM/EDX, Magnetization, PCI, TDS, Laser-granulometry
	94 560: XRPD, PCI, TDS, Laser-granulometry	96 280: XRPD, PCI, TDS, Laser-granulometry	46 000: XRPD, PCI, TDS, Laser-granulometry
			96 480: XRPD, PCI, TDS, Laser-granulometry

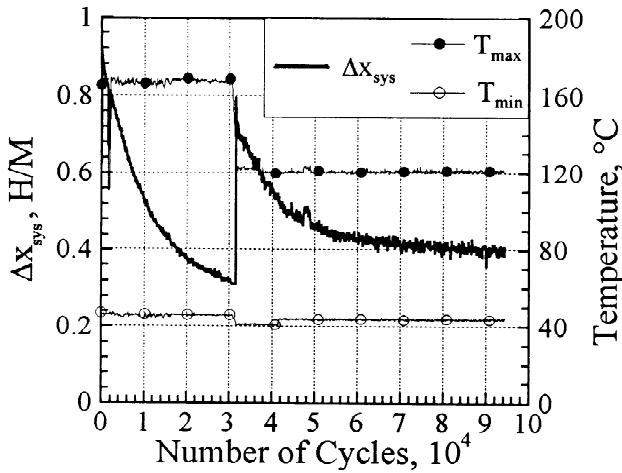


Fig. 1. Reversible system capacity (material A, $\text{LmNi}_{4.85}\text{Sn}_{0.15}$).

changes in the lattice constants a and c between the as delivered and the regenerated samples of material A, a change of the stoichiometry can be excluded).

From the system pressure changes the H/Lm ratio of the more stable hydrides formed as a consequence of disproportionation can be estimated as 3.5 compared with 2.3 in the first cycling period. This value indicates the presence of Lm–Ni–H compounds. But in the X-ray diffraction patterns, besides the AB_5 -phase, we only detected weak peaks of LmH_2 and Ni. The metallic Ni could also be detected via magnetization measurements. A medium particle size of $7 \mu\text{m}$ was derived from granulometry and SEM pictures after 31 590 cycles; it did not change during the following cycles. TDS (Fig. 3) shows two distinctive peaks (270°C , 390°C) which are in good agreement for both degraded samples.

After 31 590 cycles one reactor with degraded material was removed, the three remaining ones were regenerated in

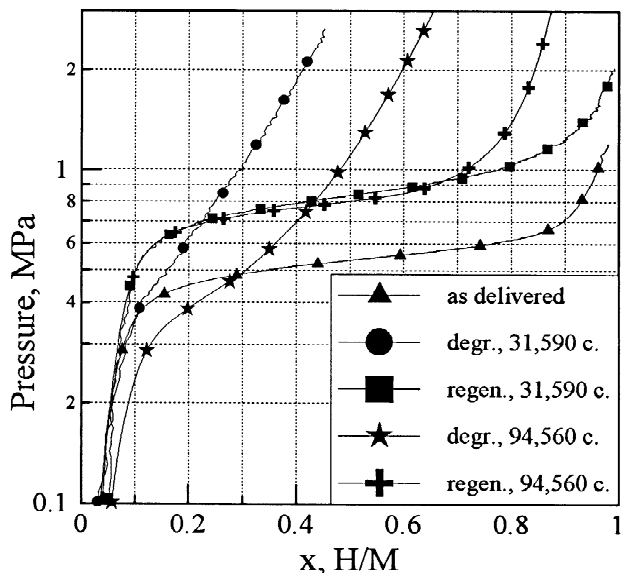


Fig. 2. Absorption PCI, 40°C (material A, $\text{LmNi}_{4.85}\text{Sn}_{0.15}$).

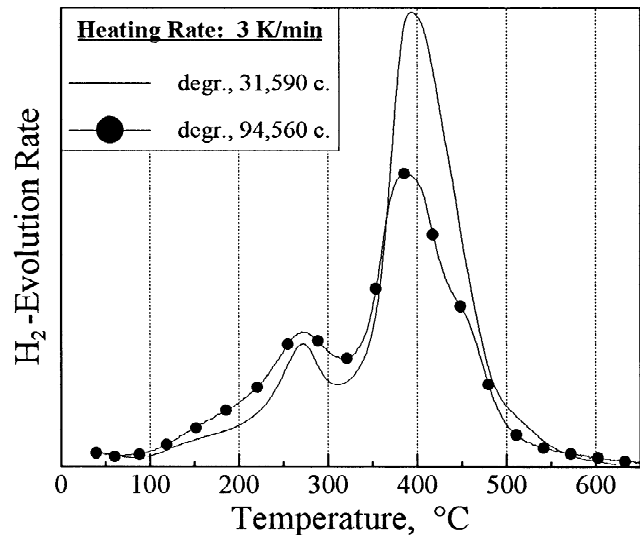


Fig. 3. Thermal desorption spectroscopy (material A, $\text{LmNi}_{4.85}\text{Sn}_{0.15}$).

an external furnace ($T=530^\circ\text{C}$; $p=1 \text{ Pa}$; $t=22.5 \text{ h}$). As described above this procedure led to a recovery of the initial hydrogen capacity. After the last cycle (No. 94,560) one reactor was regenerated in three steps at 300°C , 400°C and 500°C in the PCI device. Each step lasted 24 h and the pressure was kept at 1 Pa. After every step, the sample was cooled down to 60°C for a PCI measurement. Already after the second step, the absorption equilibrium pressure and the plateau slope reached their final values but the hydrogen capacity was still too small and the hysteresis too large. Though the third step led to an improvement of capacity and hysteresis, the original value of the hydrogen capacity was not quite reached. This may indicate that higher temperatures (probably $550\text{--}600^\circ\text{C}$) are needed for a complete recovery.

3.2. $\text{LmNi}_{4.49}\text{Co}_{0.1}\text{Mn}_{0.205}\text{Al}_{0.205}$ (material B)

In Table 1 some important data are summarized on the cycling and other investigations of material B. Fig. 4 shows the development of the reversible system capacity. The degradation rate for the first 20,000 cycles after regeneration (cycles no. 33 850–54 000) is low (7.7×10^{-6} H/M per cycle), compared to the first cycling period (2.3×10^{-5} H/M per cycle) due to the reduced cycling temperatures. As in the first period, a remaining capacity of $\Delta x_{\text{sys}}=0.41$ H/M is reached.

PCIs of material B (Fig. 5) are similar to the ones of material A. Again regeneration leads to reproducible PCIs with an equilibrium pressure $p_{\text{eq, reg}}=0.41 \text{ Mpa}$. As with material A, the value of the as delivered sample could not be achieved although we could not find significant changes in the lattice constants a and c between the as delivered and the regenerated samples. The degraded samples have shorter and steeper plateaus but their overall capacity is less affected than with materials A and C.

The H/Lm ratio of more stable hydrides in the degraded

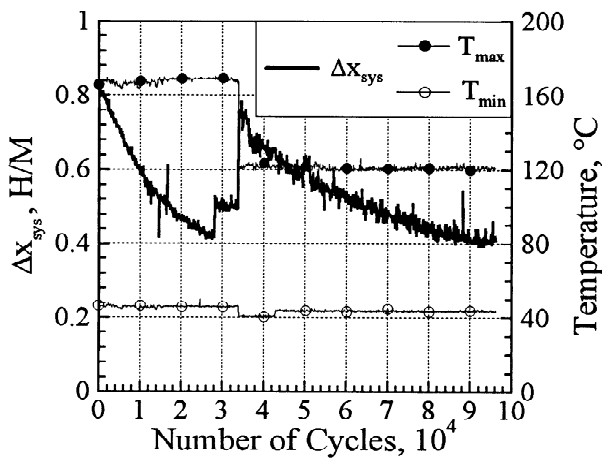


Fig. 4. Reversible system capacity (material B, $\text{LmNi}_{4.49}\text{Co}_{0.1}\text{Mn}_{0.205}\text{Al}_{0.205}$).

material is calculated as 3.6 after the second cycling period (cycles no. 33 850–96 280) in comparison to a value of 2.5 after the first period, which indicates the presence of Lm–Ni–H compounds. But in the X-ray diffraction pattern of the degraded sample we only detected the presence of LmH_2 and Ni. TDS after 96 280 cycles shows two peaks at 270 °C and 420 °C which indicate again the dissociation of two distinctive hydrides. After 33,850 cycles only one maximum at 560 °C had been detected. This may indicate the presence of only one stable hydride at this time which is also supported by the lower H/Lm ratio of 2.5 after the first degradation period. The medium particle size of 6 μm (derived from granulometry and SEM pictures after 33 850 cycles) was confirmed after 96 280 cycles.

The first regeneration was performed in situ ($T=450$ °C; $p=1$ Pa; $t=72$ h). As with material A, after the end of

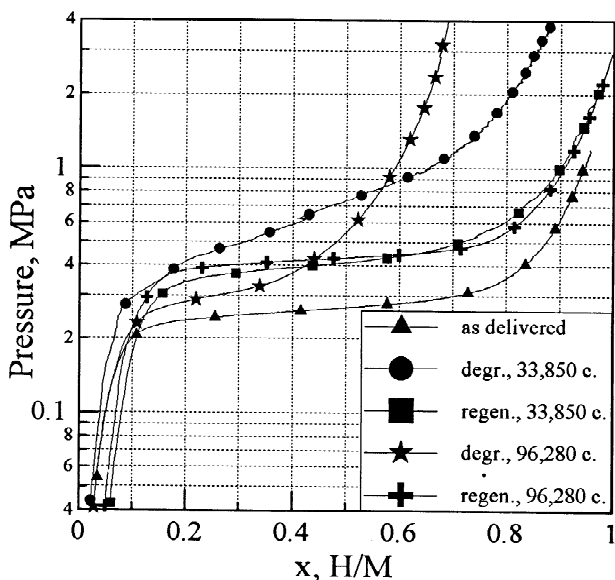


Fig. 5. Absorption PCI, 60 °C (material B, $\text{LmNi}_{4.49}\text{Co}_{0.1}\text{Mn}_{0.205}\text{Al}_{0.205}$).

cycling (96 280 cycles) one reactor was regenerated in three steps at 300 °C, 400 °C and 500 °C in the PCI device. Each step lasted 24 h and the pressure was kept at 1 Pa. After every step PCI measurements were carried out at 60 °C. Already after the second step the hydrogen capacity returned to its original value but the third step led to a further decrease of the equilibrium pressure and the plateau slope. So 500 °C is considered an adequate temperature for the complete recovery of material B.

3.3. $\text{LmNi}_{4.08}\text{Mn}_{0.62}\text{Al}_{0.1}\text{Co}_{0.2}$ (material C)

In Table 1 some important data are summarized on the cycling and other investigations of material C. Fig. 6 shows a high degradation rate (6.4×10^{-5} H/M per cycle) at the beginning of the last cycling period (cycles no. 46 100–49 100). The reversible system capacity decreased to a value of $\Delta x_{\text{sys}}=0.23$ H/M after about 80 000 cycles and then remained constant. Material C thus shows the worst degradation of the three investigated alloys. This can also be derived from the PCI illustrated in Fig. 7. The PCIs of the three degraded samples do not show a phase transition behaviour any more. However after regeneration the most important parameters such as hydrogen capacity, equilibrium pressure and plateau slope return to about their original values. The last regeneration after 96 480 cycles ($T=650$ °C; $p=1$ Pa; $t=3$ h) was the most successful one. The reached equilibrium pressure of $p_{\text{eq,reg}}=0.56$ MPa was even lower than for the as-delivered sample ($p_{\text{eq},0}=0.66$ MPa).

For the regenerated samples the X-ray diffraction patterns (Fig. 8 indicate only the original AB_5 -phase. For the degraded samples two other phases (LmH_2 and Ni) can be identified. The presence of elementary Ni was also confirmed by magnetization measurements. The severe broadening of the obtained peaks indicates both a strain and a decrease of particle size of the crystallites. The

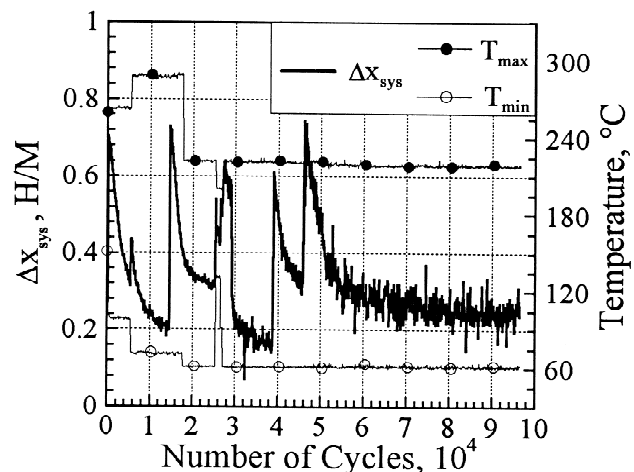


Fig. 6. Reversible system capacity (material C, $\text{LmNi}_{4.08}\text{Mn}_{0.62}\text{Al}_{0.1}\text{Co}_{0.2}$).

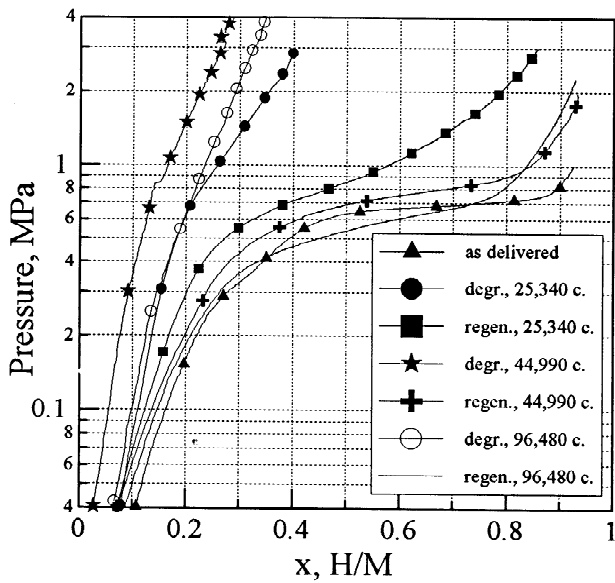


Fig. 7. Absorption PCI, 130 °C (material C, $\text{LmNi}_{4.08}\text{Mn}_{0.62}\text{Al}_{0.1}\text{Co}_{0.2}$).

medium particle size of about 8.5 μm (measured after 25 340 and 46 000 cycles) remained constant to the end of cycling.

The peaks of a TDS experiment after 46 000 cycles ($T_1=310\text{ °C}$, $T_2=550\text{ °C}$) were almost reproduced ($T_1=310\text{ °C}$, $T_2=545\text{ °C}$) after the end of cycling. This indicates the formation of well-defined hydrides that are thermodynamically more stable than LmNi_5H_6 and is in good agreement with the fact that the stability of Lm-Ni-H compounds decreases with increasing H/Lm ratio [13,14].

The comparison of the different regeneration procedures (see Table 1 Fig. 7) shows that already with an annealing temperature of 450 °C over about 25 h satisfactory results can be obtained even though the original value of the

equilibrium pressure is not reached. This is the case for an annealing temperature of 650 °C over a period of 3 h.

4. Conclusions

From the experimental investigations the following conclusions can be drawn.

(1) Depending on alloy composition and cycling temperature, significant losses of hydrogen capacity can be observed during long-term cycling in closed systems. Furthermore other material properties are also affected by the degradation. Plateau slope, equilibrium pressure (which is taken at the middle of the plateau region) and hysteresis increase. These changes might be crucial for the performance of thermodynamic devices with different coupled materials. In those devices an occasional regeneration of the built-in materials may be inevitable.

(2) The decrease of the reversible system capacity Δx_{sys} slows down exponentially and Δx_{sys} reaches a limiting value that depends on the material and the cycling conditions.

(3) The particle size decreases in the first hundred cycles [15] until an equilibrium value of 6–9 μm is reached, where the surface tension and the strains in the bulk resulting from hydrogenation balance each other.

(4) As contamination in the used closed system can be excluded, the only possible cause for the degradation is a disproportionation of the original alloy into Lm -enriched Lm-Ni compounds and elementary Ni . The H/Lm ratio in the degraded samples and the TD-spectra suggests the formation of two stable (compared with the reversible AB_5H_6) hydrides (LmH_2 and another Lm-Ni-H compound). With XRPD only LmH_2 and Ni were detected as supplementary phases. The presence of elementary Ni was also proved by magnetization measurements [11]. Considering the thermodynamic stability of the AB_5 compounds involved [14] they are stable also without hydrogen. But in the Lm-Ni-H system the desired LmNi_5H_6 hydride is much less stable than other compounds with a lower H/Lm ratio (viz. $\text{Lm}_2\text{Ni}_7\text{H}_{10}$, $\text{LmNi}_2\text{H}_{4.5}$, LmH_2). The self-diffusion that is required for such a decomposition of the alloy normally does not occur at temperatures below 300 °C. This contradiction might be resolved by assuming that local distortions during (de-)hydrogenation ease the diffusion of metal atoms along stacking defects and dislocations. Further theoretical work is required to resolve this problem.

(5) For the three investigated alloys a regeneration temperature of 500 °C (at a pressure of 1 Pa) is considered to be high enough to achieve a complete recovery of the relevant properties of the alloys. The regeneration procedure should maintain the maximum temperature for some hours. It is not yet possible to give reliable values for the minimum time necessary.

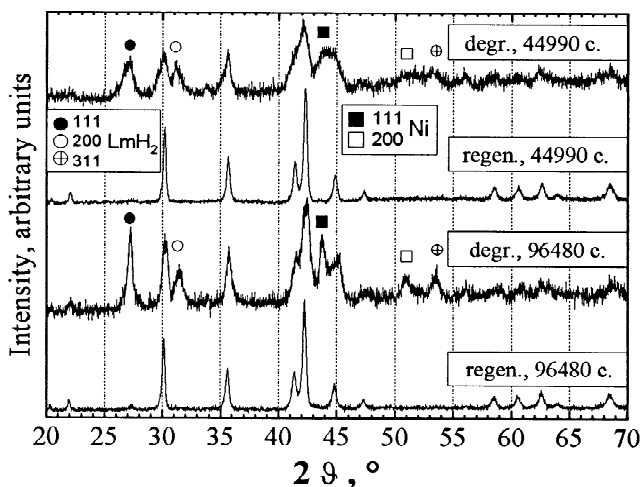


Fig. 8. X-ray diffraction patterns (material C, $\text{LmNi}_{4.08}\text{Mn}_{0.62}\text{Al}_{0.1}\text{Co}_{0.2}$, dehydrogenated).

Acknowledgments

The authors are very grateful to various laboratories of the Max-Planck-Institut für Metallforschung in Stuttgart (especially to M. Thomas) for their support with XRPD, SEM-EDX and laser granulometry experiments and to T. Magorian-Friedlmeier for her careful reading of the manuscript. This work was supported by the Deutsche Forschungsgemeinschaft (DFG) in the frame of Sonderforschungsbereich 270 Hydrogen as an Energy Carrier.

References

- [1] G. Sandrock, S. Suda and L. Schlapbach in Topics in Applied Physics, *Hydrogen in Intermetallic Compounds II*, Vol. 67, Springer, Berlin, 1992, p. 197.
- [2] S. Suda, Y. Komazaki, H. Narasaki and M. Uchida, *J. Less-Common Met.*, 172–174 (1991) 1092.
- [3] R. Werner and M. Groll, *J. Less-Common Met.*, 172–174 (1991) 1122.
- [4] M. Groll, A. Isselhorst and M. Wierse, *Int. J. Hydrogen Energy*, 19 (1994) 507.
- [5] A. Isselhorst and M. Groll, *Proc. Int. Conf. Energy and Environment*, 8–10 May 1995, p. 291.
- [6] M. Groll and A. Isselhorst, *Proc. Symp. Solid Sorption Refrigeration, Paris*, 18–20 Nov. 1992, p. 193.
- [7] D. Chandra, S. Bagchi, S.W. Lambert, W.N. Cathey, R.C. Lynch and R.C. Bowman Jr., *J. Alloys Comp.*, 199 (1993) 93.
- [8] V.Z. Mordkovich, N.N. Korostyshevsky, Yu.K. Baytchok, E.I. Mazus, N.V. Dudakova and V.P. Mordovin, *Int. J. Hydrogen Energy*, 15 (1990) 723.
- [9] Y. Josephy, E. Bershadsky and M. Ron, *J. Less-Common Met.*, 172–174 (1991) 997.
- [10] S.W. Lambert, D. Chandra, W.N. Cathey, F.E. Lynch and R.C. Bowman Jr., *J. Alloys Comp.*, 187 (1992) 113.
- [11] G. Friedlmeier, A. Manthey, M. Wanner and M. Groll, *J. Alloys Comp.*, 231 (1995) 880.
- [12] G. Friedlmeier, M. Schaaf and M. Groll, *Z. Phys. Chem.*, 183 (1994) 185.
- [13] J.I. Han and J.Y. Lee, *Int. J. Hydrogen Energy*, 13 (1988) 577.
- [14] H.J. Ahn and J.Y. Lee, *Int. J. Hydrogen Energy*, 16 (1991) 93.
- [15] J. Kallweit, *Ph.D. Thesis*, University of Stuttgart 1994.